An Experimental Study of the Acoustic Field of a Single-Cell Piezoelectric Micromachined Ultrasound Transducer (PMUT)

Bibhas Nayak*, Harshvardhan Gupta*, Kaustav Roy*, Anuj Ashok*, Vijayendra Shastri*, Rudra Pratap*
*Centre for Nano Science and Engineering
Indian Institute of Science
Bangalore, India
bibhasnayak@iisc.ac.in, bibhasn@gmail.com

2020 5th IEEE International Conference on Emerging Electronics (ICEE) | 978-1-7281-8660-3/20/$31.00 ©2020 IEEE | DOI: 10.1109/ICEE50728.2020.9777041

***Abstract*—Piezoelectric micromachined ultrasound transducers (PMUTs) have gained popularity in the past decade as acoustic transmitters and receivers. As these devices usually operate at resonance, they can deliver large output sound pressures with very low power consumption. This paper explores the influence of the transmitter's packaging on the radiated acoustic field in air. We run simplified axisymmetric numerical models to observe the change in the acoustic field and directivity with respect to the device's package dimensions. The simulations demonstrate a notable change in the directivity of transmitter based on the size of the baffle. Experimental measurements are carried out to validate the simulations, which can prove useful in designing packages for transmitters to meet application specific requirements.**

***Index Terms*—PMUT, directivity, acoustic field, air-coupled, ultrasound, diffraction**

I. Introduction

A piezoelectric micromachined ultrasound transducer or PMUT is typically a multilayered MEMS structure, fabricated by deposition and patterning of its constituent piezoelectric and electrode films on a structural layer, followed by the release of its vibrating element, generally a diaphragm by backside etching [1]. Its piezoelectric nature allows it to be used for both transmitting and receiving ultrasound. The operating frequencies of PMUTs generally range from a few tens of kHz to hundreds of MHz. With a small footprint, low operating voltage and low power draw, PMUTs find use in applications such as medical imaging [2], photoacoustics [3], range finding [4], non destructive evaluation [5], fingerprint sensing [6], density sensing [7] and data-over-sound [8].

The performance requirements from the transducer are generally dictated by the application. Apart from frequency response, output pressure and sensitivity, the directivity of the transducer can also influence its performance. For applications such as range-finding, a highly directive, on-axis radiation pattern is desirable. In contrast, proximity sensing and data-over-sound applications may benefit from a wider or omnidirectional pattern.

The packaging of a single PMUT is not a widely explored area in the field of ultrasound. There has been some work on widening the directivity of piston-like ultrasonic transducers with 3D printed baffles [9]. Other studies deal with generating highly directional ultrasonic radiation from stepped circular plates [10]. Additionally, the field of audio reproduction has generated a fair amount of literature on the shape and size of speaker cabinets [11]–[13] in which the dimensions of the speaker cabinet arguably play an important role in the directivity and frequency response at a desired listening position.

The cause behind the aforementioned influences is attributed to the interference caused by diffraction of sound around the speaker cabinet [14]. In particular, it is the diffraction of sound from the frontal edges of the cabinet that can alter the radiated acoustic field. The interference introduces changes to the frequency response at the listener's position and this is often regarded as unwanted colouring of the sound. It simultaneously modifies the radiation pattern of the speaker in the resulting sound field. This is one of the reasons why some high-fidelity audio systems have complex or unconventional shapes for their speaker cabinets.

In this paper, we highlight the effects of the package dimensions on the radiation pattern of a PMUT coupled with air. Using finite element simulations, we visualize the acoustic field generated by a PMUT for three different baffle sizes. The simulated results are validated with experimental measurements, using a reference microphone and an acoustic field scanning setup.

II. Theory

A. Radiation from a circular piston on an infinite baffle

The model of a piston mounted on a rigid infinite baffle is often used for its simplicity in understanding the directivity of a loudspeaker, especially due to the piston-like motion of the conventional loudspeaker diaphragm

[12]. The directivity $D(\theta)$ of a circular piston represents its radiation across different angles of observation. It is mathematically written as

$$D(\theta) = \frac{2J_1(ka\sin(\theta))}{ka\sin(\theta)}, \tag{1}$$

where J_1 is the Bessel function of the first kind, k is the angular wavenumber of radiated waves, a is the radius of the piston and θ is the angle of observation [15]. However, this expression faces problems with raised baffles on an infinite plane, where diffraction effects alter the primary source's directivity due to interference from newly formed secondary sources along the baffle's edges.

B. Diffraction of Sound

Diffraction is understood as the bending of travelling waves upon interaction with a discontinuity or obstacle that has dimensions comparable to their wavelength [16]. According to Huygens principle, diffraction causes the obstacle to act as a secondary source of spherical waves. In everyday scenarios, this phenomenon enables a person talking behind a tree or the bends of a hallway to be audible. In our case, the edges of the die and printed circuit board (PCB) of the PMUT can act as new secondary sources. Depending on their dimensions, these new sources can interfere with the transducer's acoustic radiation and alter its directivity.

III. Simulation

A. Simulation setup

A 2D axisymmetric finite element model (FEM) of the PMUT was simulated in COMSOL to observe baffle diffraction. Figures 1 and 2 illustrate the geometry of the FEM model. In Fig. 1, the PMUT with its package is placed on an infinite baffle, radiating into a space of 2π steradian with axisymmetry. The radiation space of 10 cm terminates into an absorbing, perfectly matched layer (PML) which simulates an anechoic environment. Figure 2 shows the PMUT placed on a PCB, in which the device layer is 10 µm thick with a radius of 1 mm. On the device layer lies a 650 nm thick PZT layer that has a residual tensile stress of 300 MPa. The handle layer which serves as the die's baffle is 650 µm thick. The PMUT is placed over a PCB that is 1 mm thick and contains a 1.5 mm radius hole underneath the PMUT.

In our simulation, the die's baffle diameter is kept fixed at 4.5 mm while the PCB's baffle diameter is varied to observe changes in the radiation pattern.

B. Results

An eigenfrequency study was carried out on the PMUT's diaphragm, which returned a fundamental resonant frequency of 50.7 kHz. This was followed by a frequency domain study at resonance for a reference case where the PMUT's diaphragm was flush with the infinite baffle. For observing the influence of the package, the

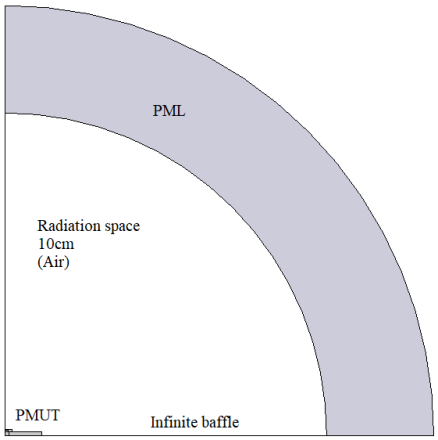

Fig. 1. 2D axisymmetric FEM model for acoustic radiation from a PMUT with the die and PCB placed on an infinite baffle.

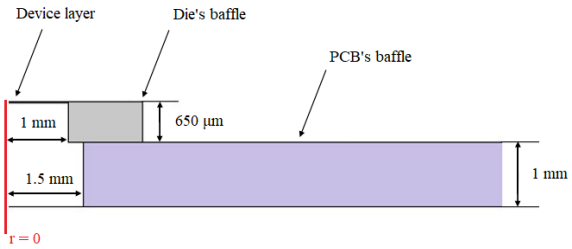

Fig. 2. Close up view of 2D axisymmetric PMUT on its PCB, with the reference axis indicated by $r = 0$.

PMUT was simulated with two different PCB baffles of diameters 8 mm and 24 mm, respectively. These diameters are equal to the breadths of the PCB baffles used in our measurements, wherein the PMUT was placed on a 12 mm x 8 mm and a 24 mm x 24 mm PCB baffle respectively.

Figure 3 depicts the sound field when the PMUT is used with an infinite baffle. Its radiation appears to be very omnidirectional with no visible pressure lobing and this is due to the lack of any diffracted waves which would have caused interference. Figure 4 represents the acoustic field of the PMUT with a PCB baffle diameter of 8 mm. A strong single lobe is observed on-axis (the vertical axis here). With a larger baffle diameter of 24 mm as shown in Fig. 5, a diminished main lobe is generated with three sidelobes around it.

The directivity of the PMUT under these different conditions is presented in Fig. 6. The behaviour of the PMUT with its diaphragm flush with an infinite baffle is quite similar to the directivity as predicted by Eq. (1). In other cases, the influence of diffraction on PMUT's directivity is quite noticeable.

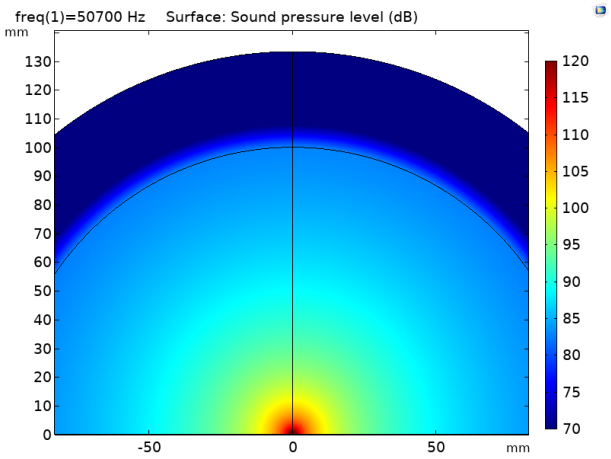

Fig. 3. Simulated acoustic radiation at 50.7 kHz with infinite baffle and with PMUT diameter of 2 mm.

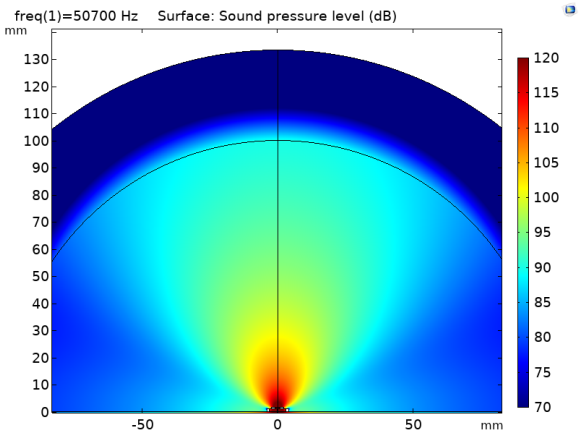

Fig. 4. Simulated acoustic radiation at 50.7 kHz with baffle diameter of 8 mm and with PMUT diameter of 2 mm.

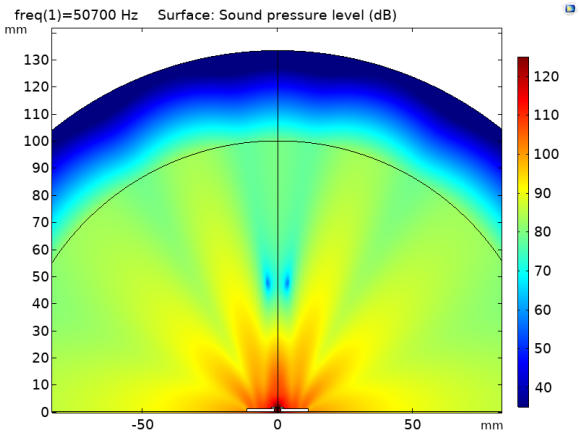

Fig. 5. Simulated acoustic radiation at 50.7 kHz with baffle diameter of 24 mm and with PMUT diameter of 2 mm.

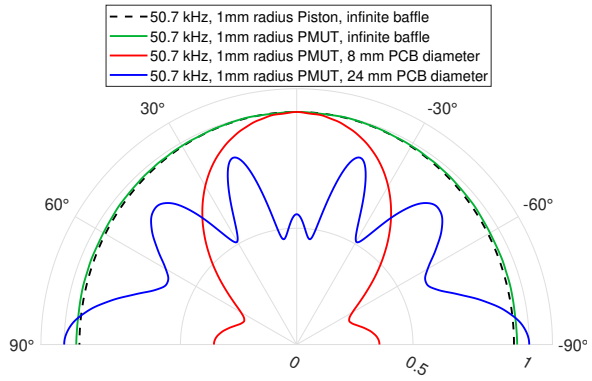

Fig. 6. Directivity of the PMUT with different baffle radii. The piston on an infinite baffle is presented as an analytical comparison.

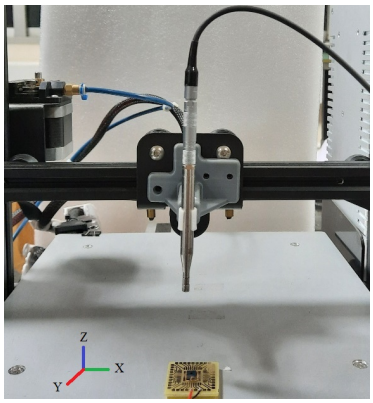

Fig. 7. 3D printer converted into a 3-axis motion system with a microphone arm, used for mapping the acoustic field of the PMUT (in picture, on a 24 mm x 24 mm PCB baffle).

IV. Experimental Measurement

A. Measurement setup

A 3D printer was modified to work as a computer-controlled 3-axis motion system for positioning a GRAS 46DP-1 reference microphone. The microphone was powered using a Brüel & Kjær Type-2829 microphone power supply. The packaged PMUT was placed on the bed of the 3D printer and driven at 50.7 kHz at $1V_{rms}$ using a Zurich Instruments MFLI lock-in amplifier. This allowed for physically mapping the sound field of the given source by sampling the pressure in a square grid pattern in front of it. To ensure minimal artifacts in the final image, the spacial sampling resolution (maximum grid dimension) was less than $\lambda/6$, where λ is the wavelength of the radiated waves. The measurement setup is shown in Fig. 7 where the PMUT is placed on the 3D-printer's bed, or the Cartesian XY plane. The acoustic field scan was performed in the XZ plane. The PMUT was oriented such that the breadth of its PCB faced the Y direction. The motion system was controlled using a LabVIEW program running on a desktop which also recorded the data from the lock-in amplifier.

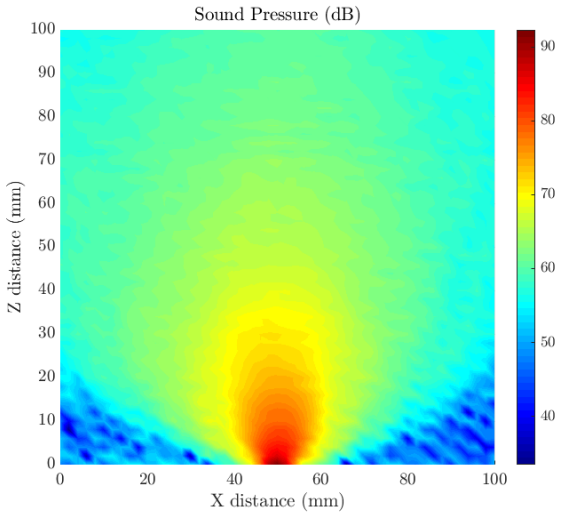

Fig. 8. Measured acoustic radiation at 50.7kHz with PCB dimensions of 12 mm x 8 mm and PMUT diameter of 2 mm.

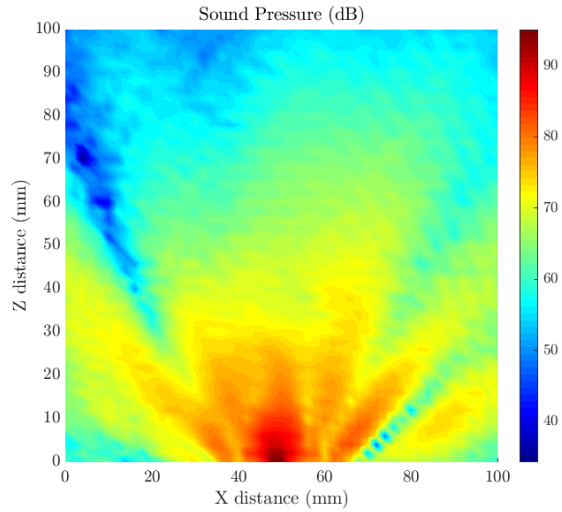

Fig. 9. Measured acoustic radiation at 50.7kHz with PCB dimensions of 24 mm x 24 mm and PMUT diameter of 2 mm.

B. Results

Using the measured scan data, the radiated acoustic field of the PMUT is plotted in Figs. 8 and 9. Since the FEM model is axisymmetric, minor differences can be observed when comparing the scanned field with the simulated field. However, the measured sound fields are in good agreement with the behaviour observed with simulations (Figs. 4 and 5), where the smaller PCB shows a prominent central lobe in comparison to the larger PCB where multiple sidelobes are caused by diffraction at the edges of the PCB. The discrepancy in the magnitude of the sound pressure levels between the simulation and measurement is due to the simulation running with COMSOL's in-built piezoelectric material (PZT-5H). A comprehensive evaluation of the PZT film used in the fabricated PMUTs has not been conducted prior to performing the simulations.

V. Conclusion

Single PMUTs are almost never packaged on an infinite baffle, and are always diced to a finite die size and bonded to a PCB package. Diffraction effects from the edges of the die and the package can significantly influence the directivity pattern of the PMUT, which has been demonstrated using acoustic field simulations and validated using measured scans of the sound field. This preliminary work highlights the importance of the package for a PMUT, which can be engineered towards application-specific requirements to control its radiation pattern.

References

[1] A. Dangi and R. Pratap, "System level modeling and design maps of PMUTs with residual stresses," *Sensors and Actuators A: Physical*, vol. 262, pp. 18–28, 2017.

[2] B. Chen, F. Chu, X. Liu, Y. Li, J. Rong, and H. Jiang, "AlN-based piezoelectric micromachined ultrasonic transducer for photoacoustic imaging," *Applied Physics Letters*, vol. 103, no. 3, pp. 1–3, 2013.

[3] A. Dangi, K. Roy, S. Agrawal, H. Chen, A. Ashok, C. Wible, M. Osman, R. Pratap, and S.-R. Kothapalli, "A modular approach to neonatal whole-brain photoacoustic imaging," *Photons Plus Ultrasound: Imaging and Sensing 2020*, vol. 11240, pp. 317 – 325, 2020.

[4] O. Rozen, S. T. Block, X. Mo, W. Bland, P. Hurst, J. M. Tsai, M. Daneman, R. Amirtharajah, and D. A. Horsley, "Monolithic mems-cmos ultrasonic rangefinder based on dual-electrode pmuts," *2016 IEEE 29th International Conference on Micro Electro Mechanical Systems (MEMS)*, pp. 115–118, 2016.

[5] H. Kazari, M. Kabir, A. Mostavi, and D. Ozevin, "Multi-frequency piezoelectric micromachined ultrasonic transducers," *IEEE Sensors Journal*, vol. 19, no. 23, pp. 11 090–11 099, 2019.

[6] H. Tang, Y. Lu, X. Jiang, E. J. Ng, J. M. Tsai, D. A. Horsley, and B. E. Boser, "3-d ultrasonic fingerprint sensor-on-a-chip," *IEEE Journal of Solid-State Circuits*, vol. 51, no. 11, pp. 2522–2533, 2016.

[7] K. Roy, H. Gupta, V. Shastri, A. Dangi, A. Jeyaseelan, S. Dutta, and R. Pratap, "Fluid density sensing using piezoelectric micromachined ultrasound transducers," *IEEE Sensors Journal*, vol. 20, no. 13, pp. 6802–6809, 2020.

[8] H. Gupta, B. Nayak, K. Roy, A. Ashok, A. Jeyaseelan A., and R. Pratap, "Development of micromachined piezoelectric near-ultrasound transducers for data-over-sound," *2020 IEEE International Ultrasonics Symposium (IUS)*, pp. 1–4, 2020.

[9] R. Kerstens, D. Laurijssen, W. Daems, and J. Steckel, "Widening the directivity patterns of ultrasound transducers using 3D printed baffles," *IEEE Sensors Journal*, vol. 17, no. 5, pp. 1454–1462, 2017.

[10] A. Barone and J. A. G. Juarez, "Flexural vibrating free edge plates with stepped thickness for generating high directional ultrasound," *The Journal of Acoustical Society of America*, vol. 51, no. 3, pp. 953–959, 1972.

[11] H. Olson, "Direct radiator loudspeaker enclosures," *Journal of Audio Engineering Society*, vol. 17, no. 1, pp. 22–29, 1969.

[12] L. Beranek and T. Mellow, *Acoustics: Sound Fields and Transducers*. Academic Press, 2012.

[13] W. M. Leach, *Introduction to Electroacoustics and Audio Amplifier Design*. Kendall Hunt, 2010.

[14] F. A. Everest, *The Master Handbook of Acoustics*. The McGraw Hill Companies, 2001.

[15] P. M. Juhl and F. Jacobsen, *Fundamentals of General Linear Acoustics*. Wiley, 2013.

[16] A. D. Pierce, *Acoustics: An Introduction to its principles and applications*. The ASA Press, 2019.